

Effects of Ethylene Glycol and Methanol on Ammonia-Induced Structural Changes of the Oxygen-Evolving Complex in Photosystem II[†]

Cheng-Hao Fang,^{‡,§} Kuo-An Chiang,^{||} Chung-Hsien Hung,[‡] Keejong Chang,[§] Shyue-Chu Ke,^{*,||} and Hsiu-An Chu^{*,‡}

Institute of Plant and Microbial Biology, Academia Sinica, Taipei, Taiwan 11529, Republic of China, Department of Chemistry, Soojow University, Taipei, Taiwan 111, Republic of China, and Department of Physics, National Dong Hwa University, Hualien, Taiwan 974-01, Republic of China

Received January 6, 2005; Revised Manuscript Received May 26, 2005

ABSTRACT: Ammonia is an inhibitor of water oxidation and a structural analogue for substrate water, making it a valuable probe for the structural properties of the possible substrate-binding site on the oxygen-evolving complex (OEC) in photosystem II (PSII). By using the NH₃-induced upshift of the 1365 cm⁻¹ IR mode in the S₂Q_A⁻/S₁Q_A spectrum and the NH₃-modified S₂ state EPR signals of PSII as spectral probes, we found that ethylene glycol has clear effects on the binding properties of the NH₃-specific site on the OEC. Our results show that in PSII samples containing 30% (v/v) ethylene glycol, the affinity of the NH₃-specific binding site on the OEC is estimated to be more than 10 times lower than that in PSII samples containing 0.4 M sucrose. In addition, our results show that the NH₃-induced upshift of the 1365 cm⁻¹ IR mode in the S₂Q_A⁻/S₁Q_A spectrum is dependent on the concentration of ethylene glycol, but not dependent on the concentration of sucrose (up to 1.5 M) or methanol (up to 5.4 M). By comparing the concentration dependence of sucrose and ethylene glycol on NH₃-induced spectral change and also by comparing the sucrose and ethylene glycol data at similar concentrations (~1 M), we conclude that ethylene glycol has a clear effect on the NH₃-induced spectral changes. Furthermore, our results also show that ethylene glycol alters the steric requirement of the amine effect on the upshift of the 1365 cm⁻¹ mode in the S₂Q_A⁻/S₁Q_A spectrum. In PSII samples containing 30% (v/v) ethylene glycol, only NH₃, not other bulkier amines (e.g., Tris, AEPD, and CH₃NH₂), has a clear effect on the upshift of the 1365 cm⁻¹ mode in the S₂Q_A⁻/S₁Q_A spectrum; in contrast, in PSII samples containing 0.4 M sucrose, both NH₃ and CH₃NH₂ have a clear effect. On the basis of the results mentioned above, we propose that ethylene glycol acts directly or indirectly to decrease the affinity or limit the accessibility of NH₃ and CH₃NH₂ to the NH₃-specific binding site on the OEC in PSII. Finally, we also applied the same approach to test whether methanol is able to compete with ammonia on its binding site on the OEC. We found that 4% (v/v) methanol does not have any significant effect on the NH₃-induced upshift of the 1365 cm⁻¹ mode in the S₂Q_A⁻/S₁Q_A spectrum and the NH₃-modified S₂ state *g* = 2 multiline EPR signal. Our results suggest that methanol is unable to compete with NH₃ upon binding to the Mn site of the OEC that gives rise to the altered S₂ state *g* = 2 multiline EPR signal.

The catalytic site of photosynthetic oxygen evolution contains a Mn₄Ca cluster that interacts closely with a redox-active tyrosine residue known as Y_Z (1–5). The Mn cluster accumulates oxidizing equivalents in response to photoinduced electron transfer reactions within PSII¹ and then catalyzes the oxidation of two molecules of water, consequently releasing one molecule of O₂ as a byproduct. The progression of the OEC goes through a cycle of five intermediates states, labeled as the S_{*n*} states (*n* = 0–4), where *n* denotes the number of stored equivalents. The S₁ state is

predominant in the dark-adapted samples. Recently, there are two reports of new X-ray crystallographic structural models of cyanobacterial photosystem II at 3.5 and 3.2 Å resolution (1, 2). These two models of the OEC agree in terms of having two moieties: one smaller moiety containing one Mn ion and one larger moiety containing the remaining Mn ions and the Ca ion. However, there are some disagreements with regard to the exact position and identity of the cations and the surrounding coordination sphere of the OEC (1, 2, 5). Higher-resolution X-ray crystallographic structures will be required to provide the complete structural model of the OEC.

[†] This work was supported by the National Science Council in Taiwan (NSC Grant 93-2311-B-001-062) and by Academia Sinica (H.-A.C.) and by the National Science Council in Taiwan (NSC Grant 93-2112-M-259-006 to S.-C.K.).

* To whom correspondence should be addressed. H.-A.C.: phone, 886-2-27899590, ext. 308; fax, 886-2-27827954; e-mail, chuha@gate.sinica.edu.tw. S.-C.K.: phone, 886-3-8633705; fax, 886-3-8633690; e-mail, ke@mail.ndhu.edu.tw.

[‡] Academia Sinica.

[§] Soojow University.

^{||} National Dong Hwa University.

¹ Abbreviations: AEPD, 2-amino-2-ethyl-1,3-propanediol; CH₃NH₂, methylamine; DCMU, 3-(3,4-dichlorophenyl)-1,1-dimethylurea; EG, ethylene glycol; EPR, electron paramagnetic resonance; ESEEM, electron spin-echo envelope modulation; FTIR, Fourier transform infrared; HEPES, *N*-(2-hydroxyethyl)piperazine-*N'*-2-ethanesulfonic acid; MeOH, methanol; OEC, oxygen-evolving complex; OTG, octyl β-D-thioglucoopyranoside; PSII, photosystem II; Q_A, primary quinone electron acceptor in PSII.

NH₃ is a structural analogue of substrate H₂O and an inhibitor of the water oxidation reaction in PSII, making it a valuable probe for the structural property of the possible substrate-binding site of the OEC of PSII (for reviews, see refs 6 and 7). EPR studies on NH₃-treated PSII samples demonstrated that alternations of the S₂ state multiline EPR signal occur when samples that have been illuminated at 200 K are subsequently "annealed" at 273 K, or when samples that are poised in the dark-stable S₁ state are illuminated at 273 K (8, 9). These results were interpreted as showing that coordination of NH₃ to the Mn site occurs after formation of the S₂ state (8, 9). An ESEEM study performed on the NH₃-altered multiline EPR signals concluded that a single NH₃-derived ligand binds directly to the Mn cluster in the S₂ state (10). In addition, this ESSEM study also provided evidence that ammonia may form an amido (NH₂) bridge between two Mn ions in place of a μ -oxo bridge (10).

Previous EPR studies demonstrated that cryoprotectants (sucrose, ethylene glycol, and glycerol) have distinct effects on the $g = 2$ multiline and $g = 4$ EPR forms of the Mn cluster in the S₂ state (6, 11). For example, sucrose stabilizes the $g = 4$ EPR form; on the other hand, ethylene glycol and glycerol enhance the $g = 2$ multiline form at the expense of the $g = 4$ EPR form. It has been suggested that cryoprotectants (sucrose, ethylene glycol, and glycerol) might have an effect on the Cl⁻ binding site on the OEC that shift the equilibrium between $g = 2$ multiline and $g = 4$ EPR forms of the Mn cluster in the S₂ state (6). However, until now, there has been no direct structural evidence to support it. In addition, one EPR study reported that in the ethylene glycol-containing medium, the affinity for NH₃ is lower than in the presence of sucrose, effectively preventing NH₃ modification of the multiline EPR signal (12). This observation was interpreted as showing that ethylene glycol might interact with the NH₃-specific binding site on the OEC (12).

Previous EPR studies also demonstrated that small alcohols affect the magnetic properties of the Mn cluster (13–16). For example, in PSII samples containing 3% (v/v) methanol, the S₂ state $g = 2$ multiline EPR signal is dominant at the expense of the $g = 4$ EPR signal. In addition, one ESEEM study on PSII samples in the presence of a series of ²H-labeled alcohols provides evidence that the small alcohol (methanol and ethanol) is located in the proximity (distance of 3.6–5 Å) of OEC and possibly serves as a direct ligand to the OEC in the S₂ state (13). However, because there is no inhibition of oxygen evolution activity up to 1 M methanol (or ethanol), the binding site for small alcohols is likely distinct from the substrate binding sites of the OEC. Alternatively, the small alcohol might initially occupy the substrate site in the S₂ state, but might be displaced by water at the higher S state of the OEC (S₃ or S₄) (16). Furthermore, one FTIR study showed that various cryoprotectants (sucrose, ethylene glycol, and glycerol) and small alcohols (methanol and ethanol) did not induce any significant changes in S₂/S₁ and S₂Q_A⁻/S₁Q_A FTIR difference spectra of PSII membranes except for the intensities of amide I bands (17). This FTIR result suggested that the two S₂ forms of the OEC that give rise to the $g = 2$ multiline and $g = 4.1$ signals have only minor differences, if any, in the structure of amino acid ligands and protein backbones (17).

Recently, we have applied FTIR difference spectroscopy to study the effect of NH₃ on structural changes of the OEC

during the S₁ to S₂ state transition (18). Our results showed that the S₂ state carboxylate mode at 1365 cm⁻¹ in the S₂Q_A⁻/S₁Q_A spectrum of the controlled samples was very likely upshifted to 1379 cm⁻¹ in that of NH₃-treated samples; however, the frequency of the corresponding S₁ carboxylate mode at 1402 cm⁻¹ in the same spectrum was not significantly affected. These two carboxylate modes have been assigned to a Mn-ligating carboxylate whose coordination mode changes from bridging or chelating to unidentate ligation during the S₁ to S₂ transition (19, 20). On the basis of the correlations between the conditions that give rise to the NH₃-induced upshift of the 1365 cm⁻¹ mode and the conditions that give rise to the modified S₂ state multiline EPR signal, we proposed that the NH₃-induced upshift of the 1365 cm⁻¹ mode is caused by the binding of the NH₃ group to the Mn site on the OEC of PSII that gives rise to the altered S₂ state multiline EPR signal (18). In this study, by using the NH₃-induced upshift of the 1365 cm⁻¹ mode in the S₂Q_A⁻/S₁Q_A spectrum and NH₃-modified S₂ state EPR signals of the OEC as spectral probes, we have characterized effects of ethylene glycol and methanol on the structural changes of the NH₃-specific site of the OEC during the S₁ to S₂ transition. The possible interaction(s) of ethylene glycol and methanol with the OEC will also be discussed.

MATERIALS AND METHODS

Sample Conditions for FTIR Measurement. Spinach OTG PSII reaction center cores (RCCs), retaining the three extrinsic polypeptides, were prepared as described in ref 21. Typical oxygen evolution rates were ~1.1–1.4 mmol of O₂ (mg of Chl)⁻¹ h⁻¹. NH₄Cl- and amine-treated PSII samples were prepared from PSII OTG RCCs. For ethylene glycol-containing PSII samples, the RCCs were washed twice with HEPES buffer [20 mM HEPES, 15 mM NaCl, and 30% (v/v) ethylene glycol (pH 7.5)]. Either NH₄Cl or other amines (CH₃NH₂, AEPD, and Tris) were added from a 1.25 M stock solution (pH adjusted to pH 7.5) to a final concentration of 100 mM or to the concentration indicated in the text. The sample suspension included 0.1 mM DCMU for the S₂Q_A⁻/S₁Q_A FTIR difference spectrum. For methanol experiments, the RCCs were washed twice with HEPES buffer [40 mM HEPES, 10 mM NaCl, and 0.4 M sucrose (pH 7.5)]. The sample suspension included 4% (v/v) methanol, 100 mM NH₄Cl, and 0.1 mM DCMU for the S₂Q_A⁻/S₁Q_A FTIR difference spectrum. Samples for FTIR measurement were prepared by centrifuging PSII OTG cores (15 min at 20 000 rpm) to produce a pellet that was then sandwiched between two CaF₂ sample windows.

Experimental Conditions for FTIR Measurement. FTIR experimental conditions were the same as those described in ref 18. Samples were cooled to 250 K by using an Oxford DN liquid nitrogen cryostat. The sample temperature was regulated to ±0.1 K with a temperature controller (Oxford ITC 502). Samples were illuminated for 4 s by a Dolan-Jenner MI 150 high-intensity illuminator with Dolan-Jenner infrared and red cutoff filters. The acquisition time for all spectra was 1 min (387 scans). The difference spectra were obtained by ratioing spectra obtained before illumination with those obtained after illumination. The spectral resolution for all spectra was 4 cm⁻¹. The multiple difference spectra were averaged to improve the signal-to-noise ratio of the spectra.

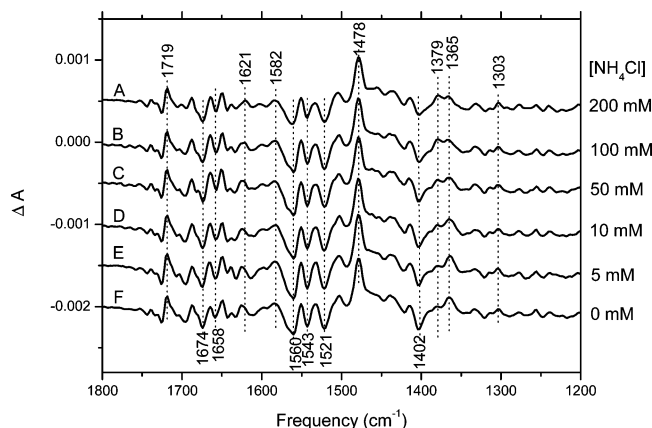


FIGURE 1: Effect of increasing concentrations of NH_4Cl on the changes of $\text{S}_2\text{Q}_\text{A}^-/\text{S}_1\text{Q}_\text{A}$ spectra of NH_3 -treated PSII containing 30% (v/v) ethylene glycol as the cryoprotectant. The spectra were recorded at 250 K. The PSII samples were treated with (A) 200, (B) 100, (C) 50, (D) 10, and (E) 5 mM and (F) no addition of NH_4Cl . Each $\text{S}_2\text{Q}_\text{A}^-/\text{S}_1\text{Q}_\text{A}$ spectrum is the average of difference spectra from three to four different samples. The sample suspension also included 0.1 mM DCMU. The intensity of each spectrum has been normalized with respect to the Q_A^- band at 1478 cm^{-1} .

Conditions for EPR Measurements. EPR experiments were performed on pellets of PSII OTG core samples in a manner similar to that for FTIR samples. In the final centrifugation step, the EPR samples were prepared by centrifuging PSII OTG cores (25 min at 5880g) to produce a pellet in EPR tubes. The samples were illuminated for 1.5 min in a nonsilvered dewar in a cold ethanol bath at 250 K by the addition of dry ice. The samples were frozen in liquid nitrogen after illumination. EPR spectra were obtained at X-band using a Bruker EMX spectrometer equipped with a Bruker TE102 cavity and an Advanced Research System continuous-flow cryostat (from 3.2 to 200 K). The microwave frequency was measured with a Hewlett-Packard 5246L electronic counter. The instrument settings are shown in the figure legend.

RESULTS

Effects of Ethylene Glycol on the $\text{S}_2\text{Q}_\text{A}^-/\text{S}_1\text{Q}_\text{A}$ Spectrum of NH_3 -Treated PSII Samples. To test the possible interaction of ethylene glycol with the NH_3 -specific site on the OEC, we studied the effect of increasing concentrations of NH_4Cl on the changes in the $\text{S}_2\text{Q}_\text{A}^-/\text{S}_1\text{Q}_\text{A}$ spectra of NH_3 -treated PSII containing 30% (v/v) ethylene glycol as the cryoprotectant. The result is shown in Figure 1. As the concentration of NH_4Cl increased from 0 to 200 mM, the intensity of the carboxylate mode at 1365 cm^{-1} progressively decreased and the intensity of the positive mode at $\sim 1379\text{ cm}^{-1}$ progressively increased. In addition, the NH_3 effect is not apparent below 50 mM NH_4Cl and is not saturated even at concentrations up to 200 mM NH_4Cl (in Figure 1A, there is still a significant amount of the carboxylate mode at 1365 cm^{-1} that can be observed at 200 mM NH_4Cl). In contrast, in our previous FTIR work on PSII samples containing 0.4 M sucrose as the cryoprotectant, the upshift of the 1365 cm^{-1} mode in $\text{S}_2\text{Q}_\text{A}^-/\text{S}_1\text{Q}_\text{A}$ spectra was apparent at 5 mM NH_4Cl and was completely saturated at 100 mM NH_4Cl (18). Therefore, our results show that the concentration dependence of the NH_3 effect on the $\text{S}_2\text{Q}_\text{A}^-/\text{S}_1\text{Q}_\text{A}$ spectrum of NH_3 -treated PSII samples containing 30% (v/v) ethylene glycol is

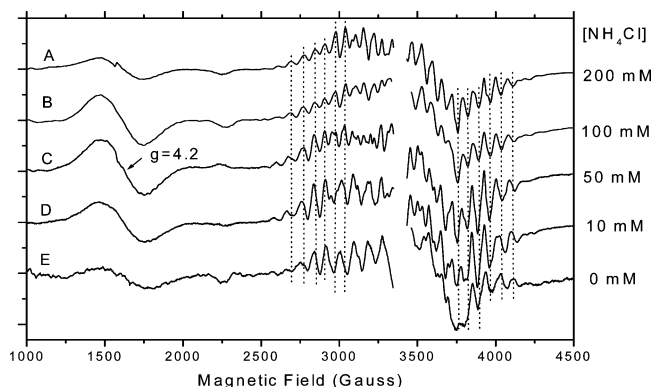


FIGURE 2: Effect of increasing concentrations of NH_4Cl on the changes of the S_2 state EPR spectra of NH_3 -treated PSII containing 30% (v/v) ethylene glycol as the cryoprotectant. The PSII samples were treated with (A) 200, (B) 100, (C) 50, and (D) 10 mM and (E) no addition of NH_4Cl . The sample suspension also included 0.1 mM DCMU. Instrument settings: microwave frequency, 9.51 GHz; modulation amplitude, 20 G at 100 kHz; temperature, 4.8 K; microwave power, 20 mW. The $g = 2$ region, which is obscured by the EPR signal of Y_D dot, has been removed for clarity. The vertical dashed lines show the positions of the hyperfine lines of the modified $g = 2$ multiline EPR signal.

significantly different from that of NH_3 -treated PSII samples containing 0.4 M sucrose as the cryoprotectant.

Figure 2 shows the effect of increasing concentrations of NH_4Cl on the changes of the S_2 state EPR spectra of NH_3 -treated PSII containing 30% (v/v) ethylene glycol as the cryoprotectant. The modified $g = 2$ multiline EPR signal was not apparent until a concentration of >50 mM NH_4Cl was reached. In addition, the intensity of the $g = 4.2$ EPR signal was increased from 0 to 50 mM and then gradually decreased from 50 to 200 mM NH_4Cl . However, there is still a significant amount of the $g = 4.2$ EPR signal that can be observed at 200 mM NH_4Cl (see Figure 2A). The behavior of the $g = 4.2$ EPR signal indicates that the NH_3 effect is not completely saturated at 200 mM NH_4Cl . In contrast, our previous EPR data on NH_3 -treated PSII samples containing 0.4 M sucrose as the cryoprotectant showed that the modified $g = 2$ multiline EPR signal was already apparent at 5 mM NH_4Cl and completely saturated at 100 mM NH_4Cl (18). In addition, the intensity of the $g = 4.2$ EPR signal was increased from 0 to 5 mM and then gradually diminished from 5 to 100 mM NH_4Cl . The intensity of the $g = 4.2$ EPR signal was completely diminished at 100 mM NH_4Cl (18). Therefore, our results show that the concentration dependence of the NH_3 effect on the alternation of S_2 state EPR signal of NH_3 -treated PSII samples containing 30% ethylene glycol is also significantly different from that of NH_3 -treated PSII samples containing 0.4 M sucrose. Moreover, our results also indicate that there is a strong correlation between the dependences on the NH_4Cl concentration that give rise to the NH_3 -induced upshift of the 1365 cm^{-1} mode in the $\text{S}_2\text{Q}_\text{A}^-/\text{S}_1\text{Q}_\text{A}$ spectrum and the condition that gives rise to the altered S_2 state multiline EPR signal in PSII samples containing 30% ethylene glycol.

Figure 3 shows the dependence of ethylene glycol concentration on the changes in the $\text{S}_2\text{Q}_\text{A}^-/\text{S}_1\text{Q}_\text{A}$ spectra of NH_3 -treated PSII. The intensity of the carboxylate mode at 1365 cm^{-1} progressively increased at the expense of the 1379 cm^{-1} mode as the concentration of ethylene glycol increased from 0 to 30% (v/v). This result clearly demonstrates that

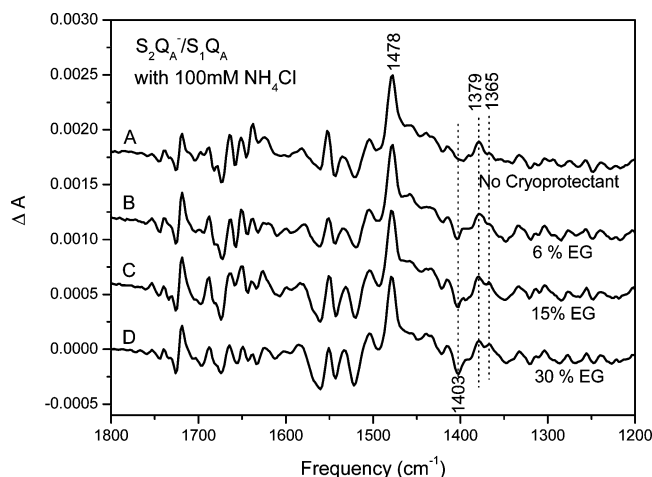


FIGURE 3: Effect of increasing concentrations of ethylene glycol on the changes of $S_2Q_A^-/S_1Q_A^-$ spectra of NH_3 -treated PSII. The PSII samples were treated with (A) no addition of ethylene glycol and (B) 6, (C) 15, and (D) 30% (v/v) ethylene glycol. Each $S_2Q_A^-/S_1Q_A^-$ spectrum is the average of difference spectra from four different samples. The sample suspension also included 0.1 mM DCMU. The intensity of each spectrum has been normalized with respect to the Q_A^- band at 1478 cm^{-1} .

ethylene glycol has a pronounced effect on the NH_3 -induced changes in the $S_2Q_A^-/S_1Q_A^-$ spectrum of NH_3 -treated PSII. In addition, we found that the overall intensity of S_2/S_1 modes (e.g., the S_1 mode at 1402 and the S_2 mode at 1365 and 1379 cm^{-1}) is significantly diminished in the $S_2Q_A^-/S_1Q_A^-$ spectra of NH_3 -treated PSII in a buffer without any cryoprotectants compared to that in buffer with ethylene glycol. The decrease in the intensity of S_2/S_1 modes in the $S_2Q_A^-/S_1Q_A^-$ spectra is correlated with the appearance of the Mn^{2+} six-line EPR signal of NH_3 -treated PSII samples in the buffer without any cryoprotectants (data not shown). Therefore, our results showed that ethylene glycol has a protective effect on the activity of the OEC in NH_3 -treated PSII samples. Figure 4 shows the effect of the increasing concentration of ethylene glycol on the changes of the S_2 state EPR signals of NH_3 -treated PSII. The intensity of the S_2 state $g = 4.2$ EPR signal progressively increased as the concentration of ethylene glycol increased. In addition, the intensity of the S_2 state $g = 4.2$ EPR signal is completely diminished in NH_3 -treated PSII samples containing no ethylene glycol (see Figure 4A). Therefore, our EPR results showed that ethylene glycol also has a pronounced effect on the NH_3 -modified S_2 state EPR signals. Furthermore, to test whether sucrose or methanol has an effect similar to that of ethylene glycol on NH_3 -induced changes of FTIR spectra, we have determined the concentration dependence of sucrose (up to 1.5 M) and methanol (up to 5.4 M) on ammonia-induced changes in FTIR spectra.² We found that sucrose (up to 1.5 M) and methanol (up to 5.4 M) do not have any significant effect on NH_3 -induced changes of FTIR spectra (data not shown). In contrast, 6% (v/v) (corresponds to ~ 1.08 M) ethylene glycol has a small but clear effect on the NH_3 -induced changes in both FTIR and EPR spectra, and this effect becomes progressively stronger as the concentration of ethylene glycol is increased (see Figures 3 and 4). Therefore,

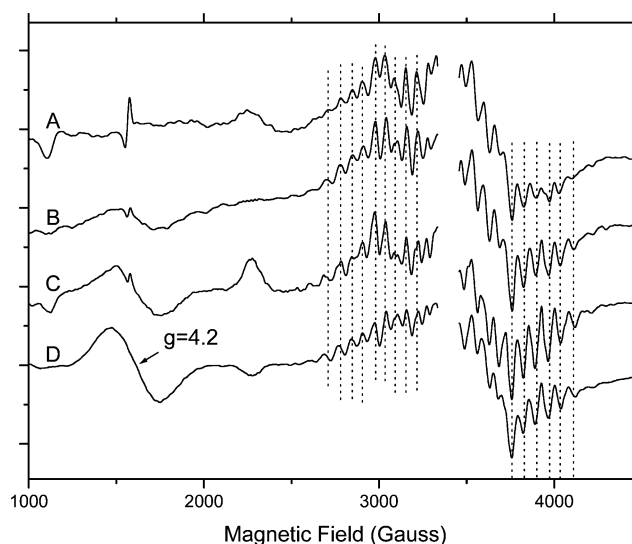


FIGURE 4: Effect of increasing concentrations of ethylene glycol on the changes of the S_2 state EPR signals of NH_3 -treated PSII. The PSII samples were treated with (A) no addition of ethylene glycol and (B) 6, (C) 15, and (D) 30% (v/v) ethylene glycol. The sample suspension also included 0.1 mM DCMU and 100 mM NH_4Cl . Instrument settings are the same as in Figure 2. The $g = 2$ region, which is obscured by the EPR signal of the Y_D dot, has been removed for clarity. The vertical dashed lines show the positions of the hyperfine lines of the modified $g = 2$ multiline EPR signal.

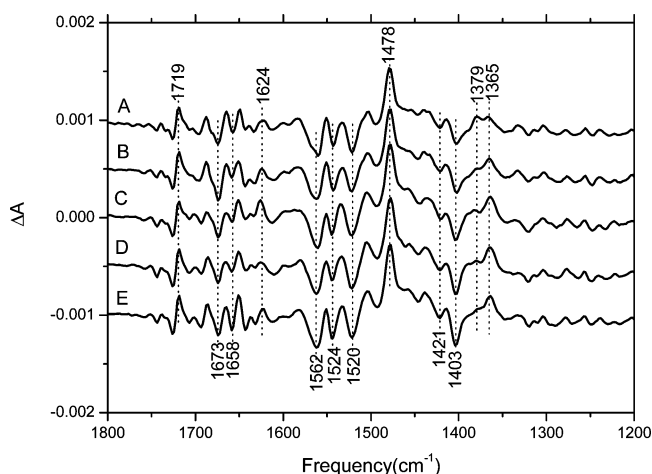


FIGURE 5: Light-minus-dark $S_2Q_A^-/S_1Q_A^-$ FTIR difference spectra of PSII samples containing 30% (v/v) ethylene glycol and 100 mM (A) NH_4Cl , (B) CH_3NH_2 , (C) AEPD, (D) Tris, and (E) NaCl. The sample suspension also included 0.1 mM DCMU. The FTIR measurement was performed at 250 K. The spectra are the average of three to four difference spectra. The intensity of each spectrum has been normalized with respect to the Q_A^- band at 1478 cm^{-1} .

by comparing the concentration dependence of sucrose and ethylene glycol on NH_3 -induced spectral change and also by comparing the sucrose and ethylene glycol data at similar concentrations (~ 1 M), we conclude that ethylene glycol has a clear effect on the NH_3 -induced changes in FTIR spectra.

Steric Requirements of the NH_3 -Binding Site in the OEC of PSII. To test the steric requirements of the NH_3 -binding site in PSII containing 30% (v/v) ethylene glycol that gives rise to the NH_3 -altered FTIR spectra, we treated the PSII samples with different primary amines (NH_3 , CH_3NH_2 , AEPD, and Tris) and studied them by FTIR. The results are shown in Figure 5. We found that only NH_3 has a clear effect on the spectral change (upshift of the 1365 cm^{-1} mode) of

² We are unable to obtain an appreciable amount of pellet for FTIR measurements from PSII samples in the buffer containing > 1.5 M sucrose under our centrifugation condition.

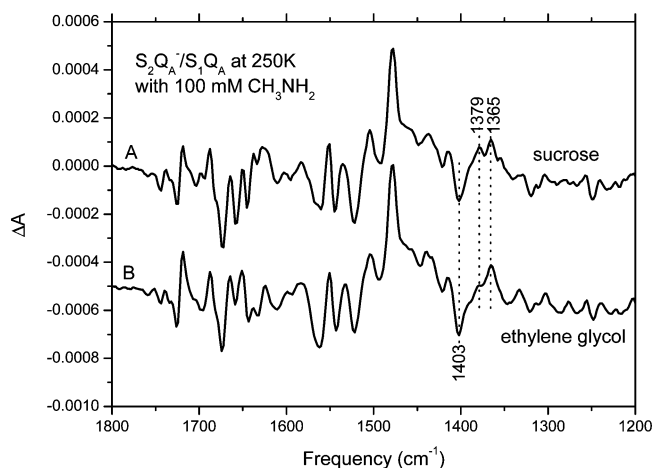


FIGURE 6: Comparison of $S_2Q_A^-/S_1Q_A$ FTIR difference spectra of CH_3NH_2 -treated PSII samples with (A) 0.4 M sucrose or (B) 30% (v/v) ethylene glycol as cryoprotectants. The sample suspension also included 100 mM CH_3NH_2 and 0.1 mM DCMU. The FTIR measurement was performed at 250 K. Spectra A and B are the average of three to four difference spectra. The intensity of each spectrum has been normalized with respect to the Q_A^- band at 1478 cm^{-1} .

the $S_2Q_A^-/S_1Q_A$ FTIR difference spectrum of PSII containing 30% (v/v) ethylene glycol. This is in contrast to our previous results on PSII samples containing 0.4 M sucrose, that being that both NH_3 and CH_3NH_2 have clear effects (18). Figure 6 shows a comparison of the CH_3NH_2 effect on the $S_2Q_A^-/S_1Q_A$ FTIR difference spectrum of PSII samples in the presence of sucrose and in the presence of ethylene glycol. We found that CH_3NH_2 induced a small but clear upshift of the S_2 state carboxylate mode at 1365 cm^{-1} of the $S_2Q_A^-/S_1Q_A$ FTIR difference spectrum of PSII in the presence of 0.4 M sucrose but not in the presence of 30% (v/v) ethylene glycol. Therefore, our result indicates that ethylene glycol significantly alters the steric requirement of amine effects on the $S_2Q_A^-/S_1Q_A$ FTIR difference spectrum of PSII samples.

Effect of Methanol on the $S_2Q_A^-/S_1Q_A$ Spectrum of NH_3 -Treated PSII Samples. To test whether methanol is able to compete with ammonia on its binding site on the OEC, we performed the $S_2Q_A^-/S_1Q_A$ FTIR difference measurement on NH_3 -treated PSII samples in the presence (Figure 7, thick line) or absence (Figure 7, thin line) of 4% (v/v) methanol. We found that methanol does not have any significant effect on the region of symmetric carboxylate stretching modes ($1450\text{--}1300\text{ cm}^{-1}$) in the $S_2Q_A^-/S_1Q_A$ FTIR difference spectrum of NH_3 -treated PSII samples. Although there are some spectral changes in the amide region, e.g., the possible amide mode at $\sim 1624\text{ cm}^{-1}$, in the $S_2Q_A^-/S_1Q_A$ spectrum of NH_3 -treated PSII in the presence of 4% (v/v) methanol (see Figure 7), these spectral changes are presumably due to the direct or indirect effect of methanol on the OEC or on the acceptor side of PSII. Figure 8 shows the S_2 state EPR spectra of NH_3 -treated PSII samples in the presence (bottom spectrum) or absence (top spectrum) of 4% (v/v) methanol. We found that methanol does not have any significant effect on the S_2 state EPR spectrum of the OEC in NH_3 -treated PSII samples either. Therefore, on the basis of our FTIR and EPR results, we found no evidence that methanol is able to compete with ammonia on its binding site on the OEC.

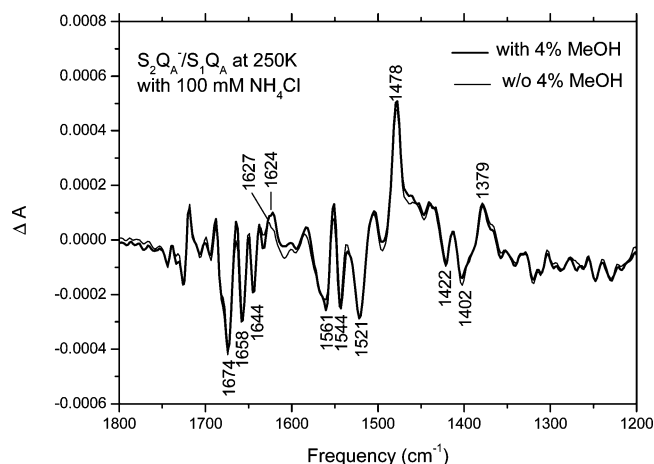


FIGURE 7: $S_2Q_A^-/S_1Q_A$ FTIR difference spectra of NH_3 -treated PSII samples in the presence of 4% (v/v) methanol. The spectra were recorded at 250 K. The PSII samples contain 0.4 M sucrose with 4% methanol (thick line) or without methanol (thin line). The sample suspension also included 100 mM NH_4Cl and 0.1 mM DCMU. These spectra represent the averages of four different spectra. The intensity of each spectrum has been normalized with respect to the Q_A^- band at 1478 cm^{-1} .

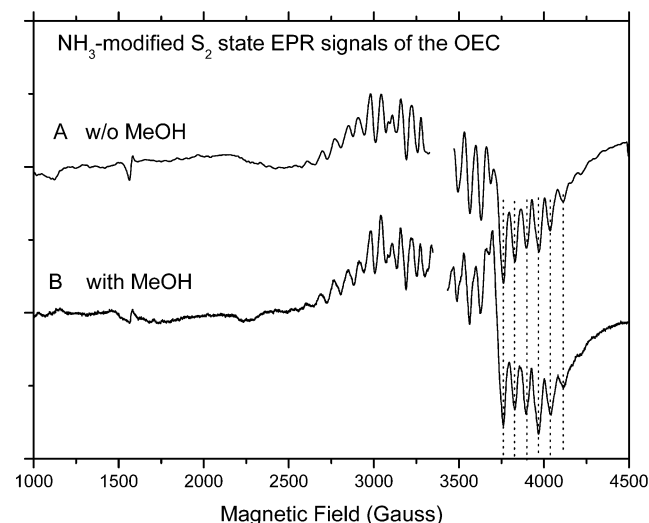


FIGURE 8: S_2 state EPR signals of the OEC in NH_3 -treated PSII samples in the absence (A) or presence (B) of 4% (v/v) methanol. The PSII samples contain 0.4 M sucrose as the cryoprotectant. The sample suspensions also included 100 mM NH_4Cl and 0.1 mM DCMU. The instrument settings are the same as in Figure 2. The $g = 2$ region, which is obscured by the EPR signal of the Y_D dot, has been removed for clarity. The vertical dashed lines show the positions of the hyperfine lines of the modified $g = 2$ multiline EPR signal.

DISCUSSION

Steric Requirement of the NH_3 -Specific Site on the OEC. A previous EPR study on PSII samples containing 30% (v/v) ethylene glycol has shown that amines other than NH_3 (e.g., Tris, AEPD, and CH_3NH_2) do not affect the S_2 state multiline EPR signal (9). The authors of this study concluded that bulkier amines such as Tris, AEPD, and even CH_3NH_2 are not able to bind to the Mn site that gives rise to the S_2 state $g = 2$ modified EPR signal because of steric factors. However, in our previous FTIR work on PSII samples containing 0.4 M sucrose, we observed that small amine CH_3NH_2 has a small but clear effect on the spectral change (e.g., upshift of the 1365 cm^{-1} mode) of the $S_2Q_A^-/S_1Q_A$

FTIR difference spectrum of PSII (18). The effects of amines on the S₂Q_A⁻/S₁Q_A FTIR difference spectrum (NH₃ > CH₃NH₂ > AEPD and Tris) are inversely proportional to their size (Tris ~ AEPD > CH₃NH₂ > NH₃). Therefore, we interpreted that the earlier EPR study was wrong in that they would have been unable to detect small populations of PSII centers having bound CH₃NH₂ (EPR spectra would have been dominated by the "normal" spectrum). However, on the basis of our FTIR results in this study, we found that in PSII samples containing 30% (v/v) ethylene glycol, only NH₃, not other bulkier amines (Tris, AEPD, and CH₃NH₂), has a clear effect on the spectral change (e.g., upshift of the 1365 cm⁻¹ mode) of the S₂Q_A⁻/S₁Q_A FTIR difference spectrum of PSII. Therefore, it is more likely that the previous disagreement is due to the different cryoprotectants used in these two studies (9, 18). In addition, there are some discrepancies in previous EPR studies with regard to NH₃-treated PSII samples at 10 mM NH₄Cl: one study reported that a normal S₂ state $g = 2$ multiline EPR signal was generated at 273 K illumination (9); however, the other studies reported that the $g = 2$ multiline EPR signal was already modified under similar conditions (12–14, 18). Their disagreements are also very likely due to the different cryoprotectants (ethylene glycol vs sucrose) used in their studies. Moreover, our results also demonstrate that the NH₃-induced upshift of the 1365 cm⁻¹ mode in the S₂Q_A⁻/S₁Q_A FTIR difference spectrum is a very sensitive probe that can detect small populations of PSII centers having bound CH₃NH₂. Therefore, this NH₃-induced FTIR spectral change is highly complementary to the NH₃-modified $g = 2$ multiline EPR signal in providing structural information about the NH₃-specific site on the OEC during the S₁ to S₂ transition.

Nature of the Interaction of Ethylene Glycol with the NH₃-Specific Site on the OEC. In this study, by using the NH₃-induced upshift of the 1365 cm⁻¹ IR mode and the NH₃-modified EPR signal as spectral probes, we found that ethylene glycol significantly alters the concentration dependence and the steric requirement for amine effects at the NH₃-specific site on the OEC of PSII. Our results are consistent with an early EPR report that in the ethylene glycol-containing medium, the affinity for the NH₃-specific site on the OEC might be lower than that in the presence of sucrose (12). To account for effects of ethylene glycol on the binding properties of the NH₃-specific site on the OEC, we propose that ethylene glycol acts directly or indirectly to decrease the affinity or limit the accessibility of NH₃ and CH₃NH₂ to the NH₃-specific site of the OEC. At present, there is no direct evidence that ethylene glycol directly interacts with the NH₃-specific site on the OEC in PSII. In addition, on the basis of the steric requirement of the amine effect on the NH₃-specific site on the OEC, the size of ethylene glycol would be too large to compete with NH₃ upon binding to this site. However, the possibility that the ethylene glycol might bind to a different site near the NH₃-specific site of the OEC, e.g., the Cl⁻ site, and decrease the affinity or limit the accessibility of NH₃ to the NH₃-specific site on the OEC in the S₂ state cannot be ruled out at this stage. Methanol might be too small to show any steric effect, and sucrose might be too large to occupy the same site to show any effect. Furthermore, our unpublished results showed that glycerol had an effect similar to that of ethylene glycol on the binding properties of the NH₃-specific site on the OEC. It is

interesting to know that the medium for the PSII crystal study contained 20% (v/v) glycerol (1). Therefore, forthcoming higher-resolution PSII crystal structures might provide the direct evidence for testing this possibility. Alternatively, the changes in structural properties of the NH₃-specific site might be due to an indirect effect of ethylene glycol on structural changes of the local protein environment around the OEC. A previous study reported that the stoichiometry of release of protons from water oxidation by the PSII core particle was restored by the addition of glycerol (24). The authors attributed this effect to the solvophobic cosolute effect of glycerol. They proposed that glycerol minimizes the (hydrophobic) protein surface in contact with water and restores and stabilizes the native protein conformation at the luminal site of PSII. Ethylene glycol might exhibit an effect similar to that of glycerol on modulating the protein conformation at the lumen site of PSII and alter binding properties of the NH₃-specific site on the OEC. In addition, a previous FTIR study showed that in the presence of 30% (v/v) ethylene glycol or 40% (v/v) glycerol in addition to sucrose, the intensities of amide I bands in S₂/S₁ or S₂Q_A⁻/S₁Q_A FTIR difference spectra were significantly larger (17). This result was interpreted as being due to the more flexible movement of the protein backbone upon formation of S₂ with the higher cryoprotectant content. On the basis of the reasons given above, we propose that ethylene glycol acts directly or indirectly to decrease the affinity or limit the accessibility of NH₃ and CH₃NH₂ to the NH₃-specific site of the OEC.

In addition, our results also demonstrate that there are strong correlations between the conditions (e.g., dependences on the NH₄Cl and ethylene glycol concentration and the steric requirement for the amine effects) that give rise to the NH₃-induced upshift of the 1365 cm⁻¹ mode in the S₂Q_A⁻/S₁Q_A spectrum and the conditions that give rise to the altered S₂ state multiline EPR signal in PSII samples containing 30% (v/v) ethylene glycol. Therefore, our results strongly imply that these two signals share the same origin: the binding of NH₃ to the NH₃-specific site in the OEC.

Effect of Methanol on the Binding Properties of the NH₃-Specific Site on the OEC. A previous ESEEM study has suggested that one methanol molecule binds to a site in the proximity of the OEC and could serve as a direct ligand to the Mn cluster (13). In addition, another ESEEM study has examined whether NH₃ and methanol can bind simultaneously at the S₂ state by titration of these two water analogues in PSII samples (16). This ESEEM study suggested that NH₃ and methanol bind in noncompetitive sites at the S₂ state and also proposed that methanol might bind to the calcium site on the OEC to displace one water ligand (16). In this study, by using the NH₃-induced upshift of the 1365 cm⁻¹ IR mode and the NH₃-modified EPR signal as spectral probes, we found that methanol does not have any significant effect on the region of symmetric carboxylate stretching modes (1450–1300 cm⁻¹) in the S₂Q_A⁻/S₁Q_A FTIR difference spectrum of NH₃-treated PSII samples or on the spectral changes of the S₂ state EPR signals. If methanol binds to the NH₃-specific site on the OEC to displace ammonia, then we should expect to see a clear effect on the NH₃-modified S₂ state EPR signals and also on the NH₃-induced upshift of the S₂ state symmetric carboxylate stretching mode in the S₂Q_A⁻/S₁Q_A spectrum of PSII. However, we did not see such effects. Therefore, our results

would indicate that methanol is not able to compete with ammonia for binding to the NH_3 -specific site on the Mn cluster. Our result is consistent with the ESEEM result (16). In addition, although the sizes of the methanol and methylamine are very similar, our results showed that only methylamine has a clear effect on the NH_3 -induced spectral changes in the $\text{S}_2\text{Q}_\text{A}^-/\text{S}_1\text{Q}_\text{A}$ spectrum of PSII. Therefore, our results indicate that, in addition to the steric factor, there might be other factors (e.g., physicochemical property of the Mn cluster) governing the selectivity of the NH_3 binding site that allows the binding of NH_3 and methylamine but excludes the binding of methanol.

In conclusion, by using the NH_3 -induced upshift of the 1365 cm^{-1} mode in the $\text{S}_2\text{Q}_\text{A}^-/\text{S}_1\text{Q}_\text{A}$ FTIR difference spectrum and the NH_3 -modified S_2 state EPR signals of PSII as spectral probes, our results demonstrate that ethylene glycol significantly alters the affinity and the steric requirement for amine effects at the NH_3 -specific site on the OEC of PSII. We propose that ethylene glycol acts directly or indirectly to decrease the affinity or limit the accessibility of NH_3 and CH_3NH_2 to the NH_3 -specific binding site on the OEC of PSII. In addition, our results suggest that methanol is unable to compete with NH_3 for binding to the NH_3 -specific site of the OEC that gives rise to the altered S_2 state $g = 2$ multiline EPR signal. Moreover, our results demonstrate that the NH_3 -induced upshift of the 1365 cm^{-1} mode in the $\text{S}_2\text{Q}_\text{A}^-/\text{S}_1\text{Q}_\text{A}$ FTIR difference spectrum very likely has the same origin as the NH_3 -modified S_2 state $g = 2$ multiline EPR signal of PSII and is complementary to the NH_3 -modified S_2 state EPR signals in providing structural information about the NH_3 -specific site on the OEC during the S_1 to S_2 transition. Future studies [e.g., X-ray crystallography (1, 2), FTIR (25–39), pulse EPR (13–16, 40, 41), or resonance Raman spectroscopy (42)] might shed some new light on the exact nature of the interaction of ethylene glycol and methanol with the OEC and also provide other new structural insights into the structural mechanism of photosynthetic water oxidation.

ACKNOWLEDGMENT

We are grateful to Prof. Richard J. Debus for critical reading of the manuscript. We are indebted to the reviewers for helpful comments on the manuscript.

REFERENCES

1. Ferreira, K. N., Iverson, T. M., Maghlaoui, K., Barber, J., and Iwata, S. (2004) Architecture of the photosynthetic oxygen-evolving center, *Science* 303, 1831–1838.
2. Biesiadka, J., Loll, B., Kern, J., Irrgang, K.-D., and Zouni, A. (2004) Crystal structure of cyanobacterial photosystem II at 3.2 Å resolution: A closer look at the Mn-cluster, *Phys. Chem. Chem. Phys.* 6, 4733–4736.
3. Sauer, K., and Yachandra, V. K. (2004) The water-oxidation complex in photosynthesis, *Biochim. Biophys. Acta* 1655, 140–148.
4. Vrettos, J. S., and Brudvig, G. W. (2004) Oxygen evolution, *Compr. Coord. Chem.* II 8, 507–547.
5. Barber, J., Ferreira, K., Maghlaoui, K., and Iwata, S. (2004) Structural model of the oxygen-evolving center of photosystem II with mechanistic implications, *Phys. Chem. Chem. Phys.* 6, 4737–4742.
6. Debus, R. J. (1992) The manganese and calcium ions of photosynthetic oxygen evolution, *Biochim. Biophys. Acta* 1102, 269–352.
7. Brudvig, G. W., and Beck, W. F. (1992) Oxidation–reduction and ligand-substitution reactions of the oxygen-evolving center of photosystem II, in *Manganese Redox Enzymes* (Pecoraro, V. L., Ed.) pp 119–141, VCH Publishers, New York.
8. Beck, W. F., de Paula, J. C., and Brudvig, G. W. (1986) Ammonia binds to the manganese site of the O_2 -evolving complex of photosystem II in the S_2 state, *J. Am. Chem. Soc.* 108, 4018–4022.
9. Beck, W. F., and Brudvig, G. W. (1986) Binding of amines to the O_2 -evolving center of photosystem II, *Biochemistry* 25, 6479–6486.
10. Britt, R. D., Zimmermann, J.-L., Sauer, K., and Klein, M. P. (1989) Ammonia binds to the catalytic Mn of the oxygen-evolving complex of photosystem II: Evidence by electron spin–echo envelope modulation spectroscopy, *J. Am. Chem. Soc.* 111, 3522–3532.
11. Zimmermann, J.-L., and Rutherford, A. W. (1986) Electron paramagnetic resonance properties of the S_2 state of the oxygen-evolving complex of photosystem II, *Biochemistry* 25, 4609–4615.
12. Andréasson, L.-E., Hansson, O., and von Schenck, K. (1988) The interaction of ammonia with the photosynthetic oxygen-evolving system, *Biochim. Biophys. Acta* 936, 351–360.
13. Force, D. A., Randall, D. W., Lorigan, G. A., Clemens, K. L., and Britt, R. D. (1998) ESEEM studies of alcohol binding to the manganese cluster of the oxygen-evolving complex of photosystem II, *J. Am. Chem. Soc.* 120, 13321–13333.
14. Evans, M. C. W., Gourovskaya, K., and Nugent, J. H. A. (1999) Investigation of the water oxidizing manganese complex of photosystem II with the aqueous solvent environment, *FEBS Lett.* 450, 285–288.
15. Deák, Z., Peterson, S., Geijer, P., Åhring, A., and Styring, S. (1999) Methanol modification of the electron paramagnetic resonance signals from the S_0 and S_2 state of the water-oxidizing complex of photosystem II, *Biochim. Biophys. Acta* 1412, 240–249.
16. Britt, R. D., Campbell, K. A., Peloquin, J. M., Gilchrist, M. L., Aznar, C. P., Dicus, M. M., Robblee, J., and Messinger, J. (2004) Recent pulsed EPR studies of photosystem II oxygen-evolving complex: Implications as to water oxidation mechanisms, *Biochim. Biophys. Acta* 1655, 158–171.
17. Onoda, K., Mino, H., Inoue, Y., and Noguchi, T. (2000) An FTIR study on the structure of the oxygen-evolving Mn-cluster of photosystem II in different spin forms of the S_2 state, *Photosynth. Res.* 63, 47–57.
18. Chu, H. A., Feng, Y. W., Wang, C. M., Chiang, K. A., and Ke, S. C. (2004) Ammonia-induced structural changes of the oxygen-evolving complex in photosystem II as revealed by light-induced FTIR difference spectroscopy, *Biochemistry* 43, 10877–10885.
19. Noguchi, T., Ono, T., and Inoue, Y. (1995) Direct detection of a carboxylate bridge between Mn and Ca^{2+} in the photosynthetic oxygen-evolving center by means of Fourier transformed infrared spectroscopy, *Biochim. Biophys. Acta* 1228, 189–200.
20. Kimura, Y., and Ono, T.-A. (2001) Chelator-induced disappearance of carboxylate stretching vibrational modes in S_2/S_1 FTIR spectrum in oxygen-evolving complex of photosystem II, *Biochemistry* 40, 14061–14068.
21. Mishra, R. K., and Ghanotakis, D. F. (1994) Selective extraction of CP 26 and CP 29 proteins without affecting the binding of the extrinsic proteins (33, 23 and 17 kDa) and the DCMU sensitivity of a photosystem II core complex, *Photosynth. Res.* 42, 37–42.
22. Boussac, A., Rutherford, A. W., and Styring, S. (1990) Interaction of ammonia with the water splitting enzyme of photosystem II, *Biochemistry* 29, 24–32.
23. Ono, T., and Inoue, Y. (1988) Abnormal S-state turnovers in NH_3 -binding Mn centers of photosynthetic O_2 evolving system, *Arch. Biochem. Biophys.* 264, 82–92.
24. Haumann, M., Hundelt, M., Jahns, P., Chroni, S., Bögershausen, O., Ghanotakis, D., and Junge, W. (1997) Proton release from water oxidation by photosystem II: Similar stoichiometries are stabilized in thylakoids and PSII core particles by glycerol, *FEBS Lett.* 410, 243–248.
25. Chu, H.-A., Debus, R. J., and Babcock, G. T. (2001) D1-Asp 170 is structurally coupled to the oxygen-evolving complex in photosystem II as revealed by light-induced Fourier transform infrared difference spectroscopy, *Biochemistry* 40, 2312–2316.
26. Chu, H.-A., Gardner, M. T., O'Brien, J. P., and Babcock, G. T. (1999) Low-frequency Fourier transform infrared spectroscopy

- of the oxygen-evolving and quinone acceptor complexes in photosystem II, *Biochemistry* 38, 4533–4541.
27. Chu, H.-A., Gardner, M. T., Hillier, W., and Babcock, G. T. (2000) Low-frequency Fourier transform infrared spectroscopy of the oxygen-evolving complex in Photosystem II, *Photosynth. Res.* 66, 57–63.
28. Chu, H.-A., Sackett, H., and Babcock, G. T. (2000) Identification of a Mn–O–Mn cluster vibrational mode of the oxygen-evolving complex in photosystem II by low-frequency FTIR spectroscopy, *Biochemistry* 39, 14371–14376.
29. Chu, H.-A., Hillier, W., Law, N. A., and Babcock, G. T. (2001) Vibrational spectroscopy of the oxygen-evolving complex and of manganese model compounds, *Biochim. Biophys. Acta* 1503, 69–82.
30. Chu, H.-A., Hillier, W., and Debus, R. J. (2004) Evidence that the C-terminus of the D1 polypeptide of photosystem II is ligated to the manganese ion that undergoes oxidation during the S₁ to S₂ transition: An isotope-editing FTIR study, *Biochemistry* 43, 3152–3166.
31. Debus, R. J., Strickler, M. A., Walker, L. M., and Hillier, W. (2005) No evidence from FTIR difference spectroscopy that aspartate-170 of the D1 polypeptide ligates a Mn ion that undergoes oxidation during the S₀ to S₁, S₁ to S₂, or S₂ to S₃ transition in photosystem II, *Biochemistry* 44, 1367–1374.
32. Kimura, Y., Mizusawa, N., Ishii, A., Yamanari, T., and Ono, T. (2003) Changes of low-frequency vibrational modes induced by universal ¹⁵N- and ¹³C-isotope labeling in S₂/S₁ FTIR difference spectrum of the oxygen-evolving complex, *Biochemistry* 42, 13170–13177.
33. Yamanari, T., Kimura, Y., Mizusawa, N., Ishii, A., and Ono, T. (2004) Mid- to low-frequency Fourier transform infrared spectra of S-state cycle for photosynthetic water oxidation in *Synechocystis* sp. PCC 6803, *Biochemistry* 43, 7479–7490.
34. Hasegawa, K., Kimura, Y., and Ono, T. (2004) Oxidation of the Mn cluster induces structural changes of NO₃[−] functional bound to the Cl[−] site in the oxygen-evolving complex of photosystem II, *Biophys. J.* 86, 1042–1050.
35. Mizusawa, N., Yamanari, T., Kimura, Y., Ishii, A., Nakazawa, S., and Ono, T. (2004) Changes in the functional and structural properties of the Mn cluster induced by replacing the side group of the C-terminus of the D1 protein of photosystem II, *Biochemistry* 43, 14644–14652.
36. Mizusawa, N., Kimura, Y., Ishii, A., Yamanari, T., Nakazawa, S., Teramoto, H., and Ono, T. (2004) Impact of replacement of D1 C-terminal alanine with glycine on structure and function of photosynthetic oxygen-evolving complex, *J. Biol. Chem.* 279, 29622–29627.
37. Noguchi, T., and Sugiura, M. (2000) Structure of an active water molecule in the water-oxidizing complex of photosystem II as studied by FTIR spectroscopy, *Biochemistry* 39, 10943–10949.
38. Noguchi, T., and Sugiura, M. (2002) FTIR detection of water reactions during the flash-induced S-state cycle of the photosynthetic water-oxidizing complex, *Biochemistry* 41, 15706–15712.
39. Noguchi, T., and Sugiura, M. (2003) Analysis of flash-induced FTIR difference spectra of the S-state cycle in the photosynthetic water-oxidizing complex by uniform N-15 and C-13 isotope labeling, *Biochemistry* 42, 6035–6042.
40. Peloquin, J. M., Campbell, K. A., Randall, D. W., Evanchik, M. A., Pecoraro V. L., Armstrong, W. H., and Britt, R. D. (2000) Mn-55 ENDOR of the S₂-state multiline EPR signal of photosystem II: Implications on the structure of the tetranuclear Mn cluster, *J. Am. Chem. Soc.* 122, 10926–10942.
41. Peloquin, J. M., and Britt, R. D. (2001) EPR/ENDOR characterization of the physical and electronic structure of the OEC Mn cluster, *Biochim. Biophys. Acta* 1503, 96–111.
42. Cua, A., Stewart, D. H., Reifler, M. J., Brudvig, G. W., and Bocian, D. F. (2000) Low-frequency resonance Raman characterization of the oxygen-evolving complex of photosystem II, *J. Am. Chem. Soc.* 122, 2069–2077.

BI050030K